Immunity, Volume *33*

Supplemental Information

Human CD14^{dim} Monocytes Patrol and Sense Nucleic Acids and Viruses via TLR7 and TLR8 Receptors

Jérôme Cros, Nicolas Cagnard, Kevin Woollard, Natacha Patey, Shen-Ying Zhang, Brigitte Senechal, Anne Puel, Subhra K. Biswas, Despina Moshous, Capucine Picard, Jean-Philippe Jais, David D'Cruz, Jean-Laurent Casanova, Céline Trouillet, and Fréderic Geissmann

Figure S1, relates to figure 1.

A : Monocyte are contained among DR+ cells (or CD115+ cells) that do not express B-cell (CD19$^-$), T-cell (CD2$^-$), NK-cell (CD56$^-$ NKp46$^-$), or granulocyte makers (CD15$^-$). Within this gate, large CD14$^+$CD16 and CD14$^+$CD16$^+$ monocytes, small CD14^{dim}CD16$^+$ monocytes and CD14$^-$CD16$^-$ DCs can be separated. To exclude cell doublets, cells were gated using Area vs Width signal intensity. All sorted cells were CD62P (AK4, APC) negative (not shown), indicating platelets were not bound to purified monocytes.
B : Hierarchical clustering of human D1 (average of triplicates) D2, and D3 samples and of the 3 mouse samples, using common genes (fold 2, 3104 genes) using the Spearman correlation similarity measure and average linkage in clustering algorithm **C :** Hierarchical clustering of all human and mouse samples, using common genes (15624 genes) using the Spearman correlation similarity measure and average linkage in clustering algorithm **D :** PCA analysis using a covariance matrix. **E :** Mouse blood monocytes were purified by flow cytometry and incubated for 2h at 37°C and 5%CO2 in complete medium alone or supplemented with LPS (0.1-100 ng/ml). **F** : Mouse blood monocytes were incubated for 18h at 37°C and 5%CO2 in complete medium alone or supplemented with LPS (10ng/ml) or a TLR7 agonist 3M13 (3ug/ml). Supernatant were collected and assayed by ELISA for the indicated cytokines. AU: arbitrary units. 'LPS induced a stronger response in Ly6c+ monocytes, but not Ly6c-. In contrast Ly6c- responded better to stimulation with the TLR7 agonist.

Figure S2, relates to figure 2.

A : Gene expression profiles of human monocyte subset, from EMBL-EBI "array express' database, Geissman_Miltenyi_Mouse. **B** : Cytokine production by monocyte subsets in response to TLR1/2 agonist PAM3CK4 was studied as described in methods. **C** : Production of IL-10 by CD14+16- and CD14+16+ monocytes after 18 and 36hrs stimulation with LPS. **D :** Allogeneic MLR. 10^5 lymphocytes were incubated with monocytes,at the indicated stimulator to effector ratio. 3HT incorporation was measured over a 18 h pulse at day 4 of coculture. **E** : mean expression of HLA-DR measured by flow cytometry and normalised by CD14+16- mo. mean ±SD; 9 donors

Figure S3, relates to figure 4.

A : Expression of TLR receptors on CD3 Tcells, CD19 B cells, CD14+CD16- and CD14-CD16+ was determined by qPCR. Values are % of PBMCS controls. **B** : Cytokine production

in response to TLR7/8 agonists. Isolated monocyte subsets (as indicated) or PBMC were stimulated with vehicle control (medium), TLR8 (3M2; 3ug/ml) or TLR7 (3M13; 3ug/ml) for 24hrs at 37oC. Supernatant was collected and cytokines (as indicated) measured via BioPlex (see methods). Data is presented as mean±SD in expression (pg/ml) from 3 independent experiments. **C, D :** The level of infection of CD14dim monocytes, CD14+monocytes, T-cells, and fibroblasts by HSV-1 was investigated using HSV-1 gB-GFP reporter virus. Infection and cytokine production was determined 18 h after exposure to HSV-1 gB-GFP (HSV1, referenced in the result section), heat-inactivated HSV-1 gB-GFP, or UV- inactivated HSV-1 gB-GFP at a multiplicity of infection (MOI) of 1. In these experimental conditions HSV-1 did not infect monocyte and T cells , but monocytes uptake the gfp-virus. **E :** infection of CD14dim monocytes, CD14+CD16+ monocytes, CD14+CD16- monocytes, and 293T cells by Measles ssRNA (-) virus, in experiments described in figure 4, was investigated by RT-qPCR using MV3/inner 1248–1268 AGCATCTGAACTCGGTATCAC and MV4/inner 1480–1500 AGCCCTCGCATCACTTGCTCT (amplicon 250 bp) (Ghosh S, et al 2001). RT performed with MV3 allows to detect the viral genome, while RT performed with MV4 allows to detect mRNA. qPCR was positive in 293T cells infected at a MOI of 1, and on an equivalent amount of the viral stock, but not in monocytes (n=≥2), suggesting a low rate of infection and/or degradation of the virus by monocytes.

Figure S4, relates to figure 5.

A : Monocyte subsets specific activation pathways. $CD14^{+}$ monocytes (right) and $CD14^{dim}$CD16+ monocytes (left) were treated 24hrs at 37oC with vehicle control (DMSO) or TLR 7/8 agonist R848 (2ug/ml), in the presence or absence of the specific MEK inhibitor PD98059 (50uM) or p38MAPK inhibitor SB-203580 (50uM). Supernatant collected and cytokines were measured by bioplex and data is presented as mean ± standard deviation in expression (pg/ml) from 3 independent experiments.
B-F : A model for TLR7/8 signallng pathway in CD14+ and CD14 dim monocyte subset showing distinct cytokine expression patterns. **B:** Schematic representation of the computational model for TLR7/8 pathway signaling in CD14+ and $CD14^{dim}$ monocyte subsets. p38 MAPK is upregulated in CD14+ monocytes, while MEK1 (and its direct target ERK) and JNK are upregulated in CD14dim monocytes. Upregulation of p38 MAPK in the CD14+ monocytes leads to activation of cJun/cFos as well as p65/p50 NF-κB, resulting in upregulated IL-6 and IL-8 expression. Upregulation of MEK1(=ERK) and JNK in the $CD14^{dim}$ monocytes leads to activation of cJun/cFos, resulting in upregulated TNF, IL-1b expression. It may be noted that TLR7/8 signaling can also activate p65/p50 NF-κB through IKK2 without the direct involvement of any MAPKs. Differentially upregulated signaling pathways or molecules are shown by thickened line and larger font size. Dotted lines show possible crosstalks between pathways. **C:** In silico simulations from the TLR7/8 computational model showing expression profiles of indicated cytokines in the CD14+ and $CD14^{dim}$ monocytes. Expression of IL-6 and IL-8 are more strongly upregulated in CD14+ monocytes (blue) whereas TNF and IL-1b are more strongly upregulated in $CD14^{dim}$ subset (red). **D** : In silico simulation : p38 MAPK is upregulated in the CD14+ subset, while JNK and MEK1(ERK) are upregulatedin the CD14 dimsubset. **E** : MEK1 inhibition in silico in the CD14+ monocyte model causes very little change in the expression of the four cytokines. On the contrary, p38 MAPK inhibition in silicoresults in downregulationof all the four cytokines, in particular IL-6 and IL-8 which may be more dependent on p38 MAPK activity. **F :** CD14 dim monocytesdisplay drastically downregulated TNF and IL-1b expression when MEK1 is

inhibited in silico. IL-6 and IL-8 also showed downregulation but to a lesser extent. In silico inhibition of p38 MAPK did not have effect on any of the cytokine simulations.

Supplemental Reference

Ghosh S, Armitage E, Wilson D, Minor PD, Afzal MA. (2001). Detection of persistent measles virus infection in Crohn's disease: current status of experimental work. Gut *48*, 748-52.

Cros, Cagnard, Woollard, et al., Supplemental figure S4.

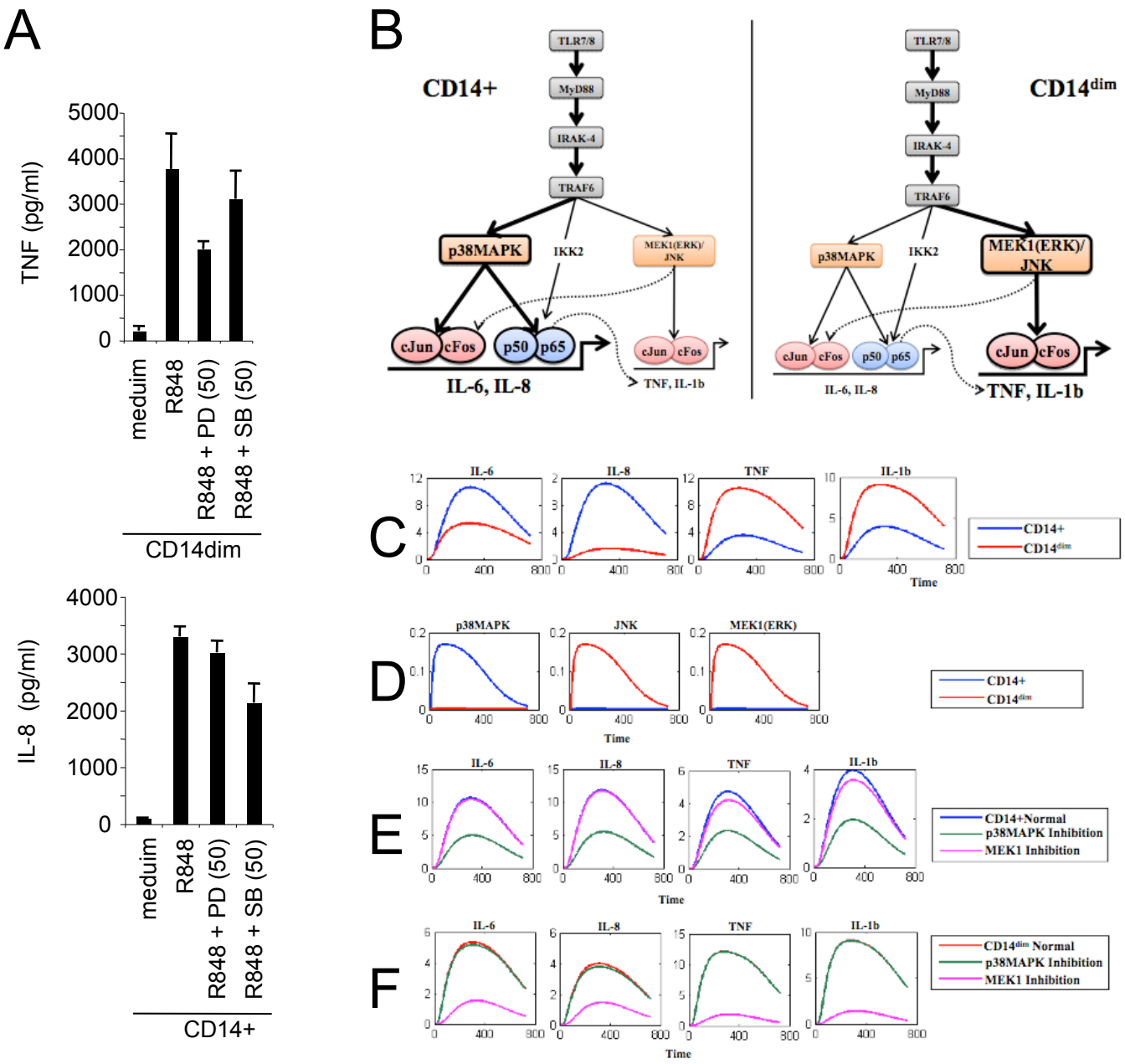

Cros, Cagnard, Woollard, et al.,
Supplemental figure S3

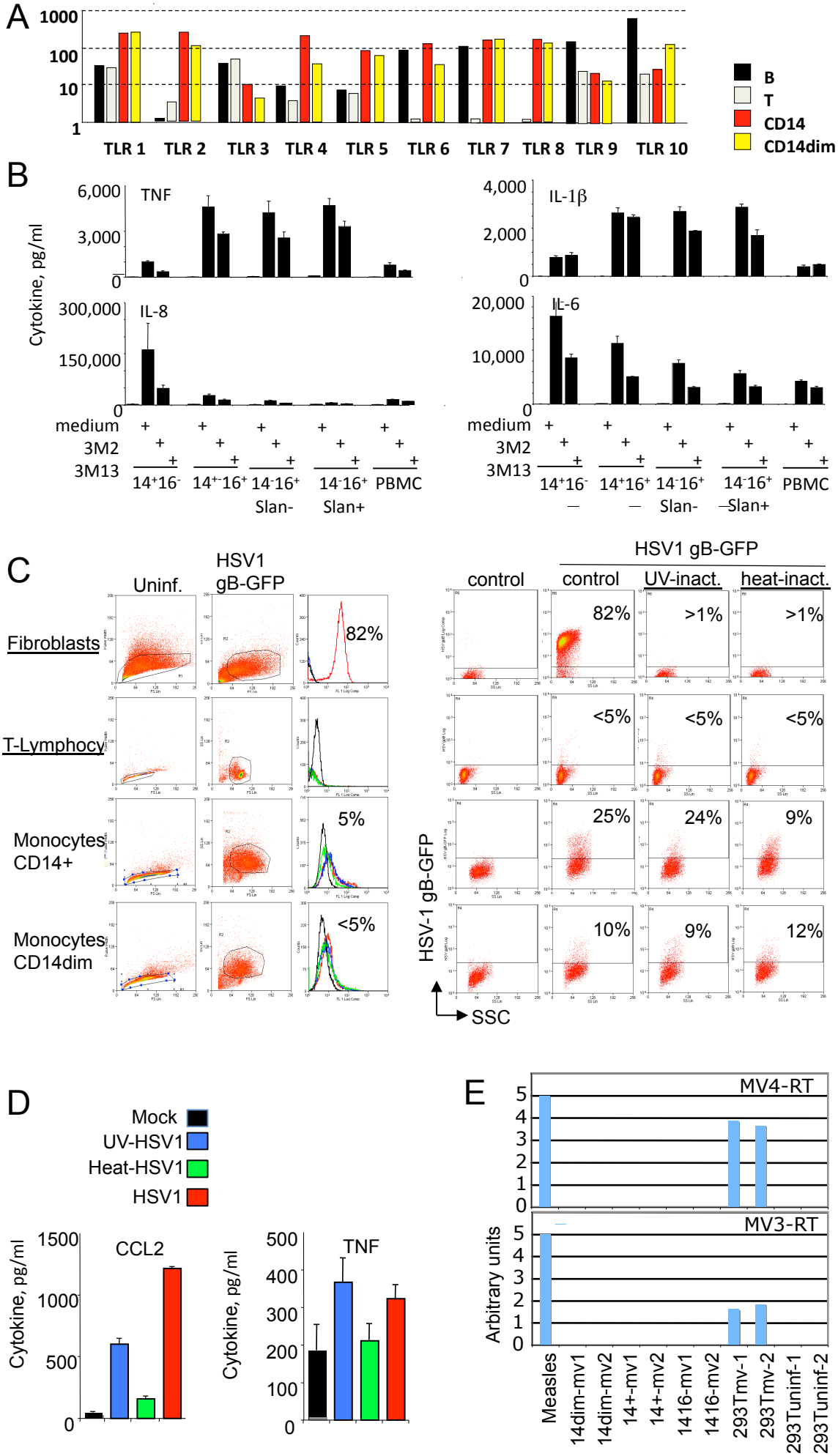

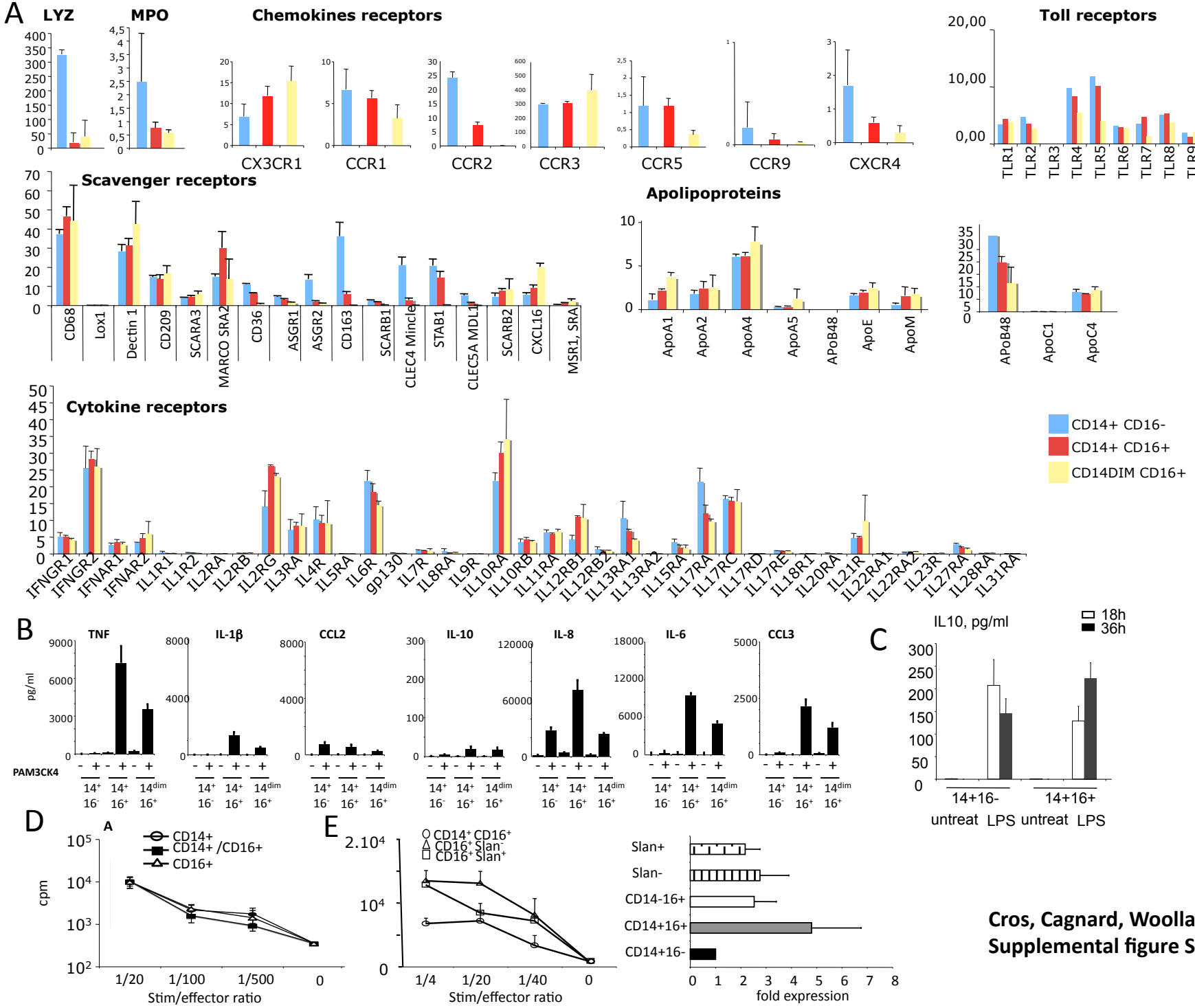

Cros, Cagnard, Woollard, et al., Supplemental figure S2.

A

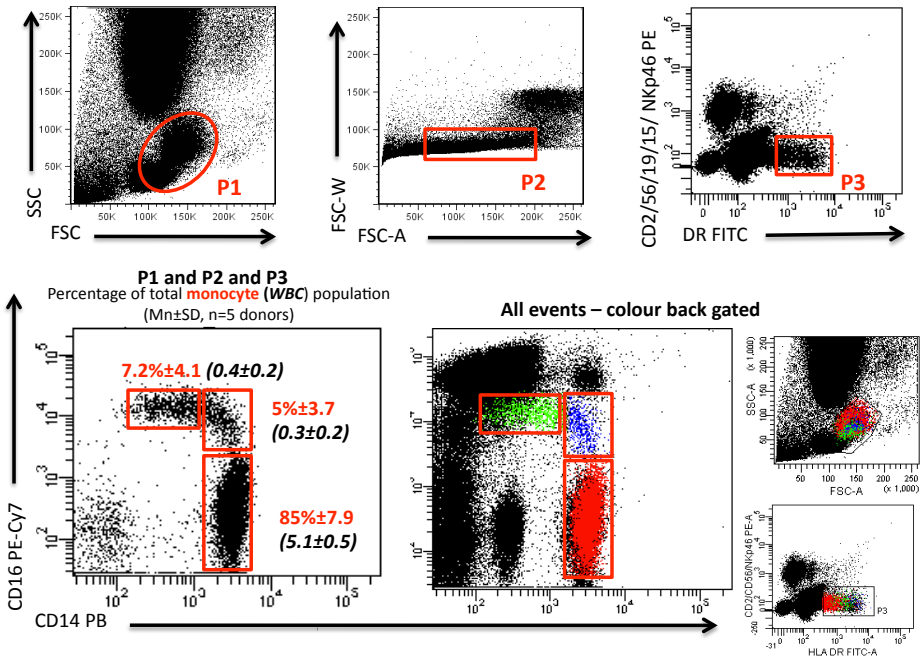
SSC
FSC
P1
FSC-W
FSC-A
P2
CD2/56/19/15/ NKp46 PE
DR FITC
P3
P1 and P2 and P3
Percentage of total monocyte (WBC) population
(Mn±SD, n=5 donors)
7.2%±4.1 (0.4±0.2)
5%±3.7
(0.3±0.2)
85%±7.9
(5.1±0.5)
CD16 PE-Cy7
CD14 PB
All events – colour back gated
SSC-A
FSC-A
HLA DR FITC-A

B

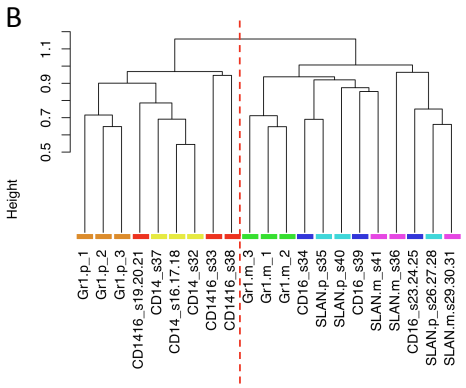
Height
Gr1.p_1
Gr1.p_2
Gr1.p_3
CD1416_s19.20.21
CD14_s37
CD14_s16.17.18
CD14_s32
CD1416_s33
CD1416_s38
Gr1.m_3
Gr1.m_1
Gr1.m_2
CD16_s34
SLAN.p_s35
SLAN.p_s40
CD16_s39
SLAN.m_s41
SLAN.m_s36
CD16_s23.24.25
SLAN.p_s26.27.28
SLAN.m.s29.30.31

C

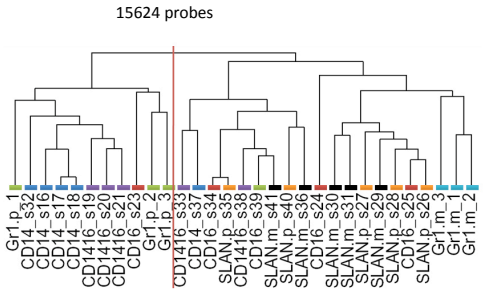
15624 probes
Gr1.p_1
CD14_s32
CD14_s16
CD14_s17
CD14_s18
CD1416_s19
CD1416_s20
CD1416_s21
CD16_s23
Gr1.p_2
Gr1.p_3
CD1416_s33
CD14_s37
CD16_s34
SLAN.p_s35
CD1416_s38
CD16_s39
SLAN.m_s41
SLAN.p_s40
SLAN.m_s36
CD16_s24
SLAN.m_s30
SLAN.m_s31
SLAN.p_s27
SLAN.m_s29
SLAN.p_s28
CD16_s25
SLAN.p_s26
Gr1.m_3
Gr1.m_1
Gr1.m_2

D

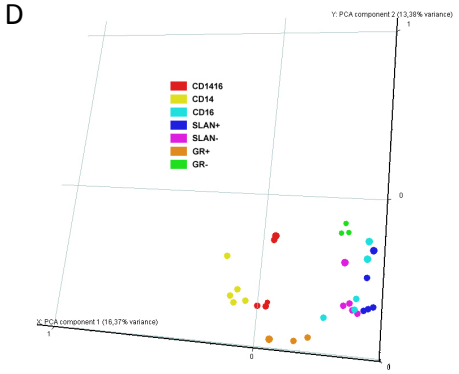
CD1416
CD14
CD16
SLAN+
SLAN-
GR+
GR-

E

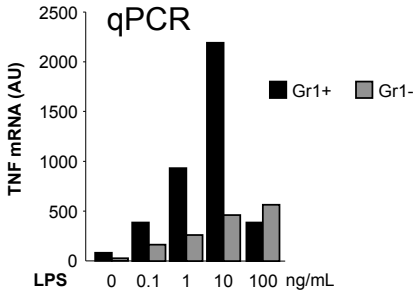
qPCR
TNF mRNA (AU)
Gr1+
Gr1-
LPS
0 0.1 1 10 100 ng/mL

F

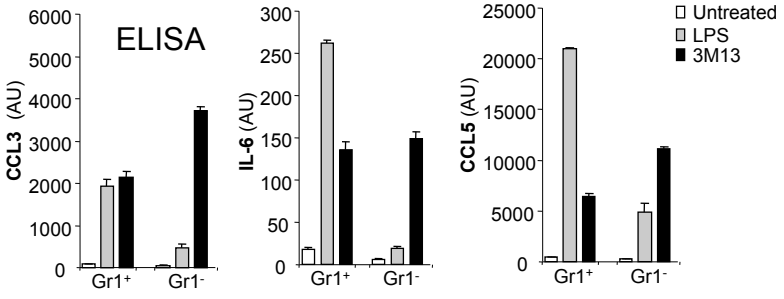
ELISA
CCL3 (AU)
IL-6 (AU)
CCL5 (AU)
Untreated
LPS
3M13
Gr1+
Gr1-

Supplemental Experimental Procedures

Monocyte phenotyping and purification

Anticoagulated (heparin) whole blood was collected from healthy volunteers after informed consent. MYD88 deficient, IRAK-4 deficient, γc-deficient patients were recruited after informed consent at the Pediatric Immuno-Hematology Unit, Hôpital Necker-Enfants Malades, Paris France. Osmotic lysis of red blood cells was performed using a ratio of 1:2.5 to lysis buffer (dH2O, NH4Cl, NaHCCO3, EDTA). RBC lysis was used to avoid activation of monocytes by ficoll density centrifugation. After lysis and washing, cells were resuspended (10µl/10^6 cells) in sorting buffer (PBS, 2mM EDTA, 0.5% BSA) and stained with anti-human antibodies (all from BD Biosciences) specific for anti-HLA-DR (TU36, FITC), anti-CD14 (M5E2, PacB), anti-CD16 (3G8, PE-Cy7), anti-CD2 (RPA-2.10, PE), anti-CD56 (MY31, PE), anti-NKp46 (BAB281, PE), anti-CD15 (VIMC6, PE) and anti-CD19 (J3-119, PE) for 15 mins at 4oC in the dark. Stained cells were filtered (70µm) and sorted on a BD FACSAria II cell sorter, using appropriate colour compensation for correcting spectral overlap and autofluorescence. Monocyte are contained among CD115+ cells, or DR+ cells, that do not express B-cell ($CD19^-$), T-cell ($CD2^-$), NK-cell ($NKp46^-$), or granulocyte makers ($CD15^-$). Within this gate, large $CD14^+CD16$ and $CD14^+CD16^+$ monocytes, small $CD14^{dim}CD16^+$ monocytes and $CD14^-CD16^-$ DCs can be separated. To exclude cell doublets, cells were gated using Area vs Width signal intensity. All sorted cells were CD62P (AK4, APC) negative, indicating platelets were not bound to purified monocytes. $CD14^+CD16^-$, $CD14^{dim}CD16^+$ and $CD14^+CD16^+$ cells were sorted into 96 well plates maintained at 4oC.

Intravital microscopy and adoptive transfer

$CD14^+CD16^-$ and $CD14^{dim}CD16^+$ human monocytes were purified from whole blood from healthy donors, as described above 'Monocyte phenotyping and purification.' Sorted cells were washed and resuspended to a concentration of $3x10^6$/ml and stained for 10mins at 37oC using Vybrant-DiD (invitrogen) (1:1000). After staining, cells were centrifuged and washed 2x and resuspended in 150ul ready for adoptive transfer to recipient mice.

Triple mutant *Cx3cr1 gfp/+ Rag2-/-* γc -/- mice were generated as previously described (Auffray et al., 2007) and maintained in our specific pathogen-free animal facility at Kings College London according to institutional guidelines, and experiments were performed under Home Office project license consent, using mice 8-12 weeks of age. Intravital microscopy was performed using a LeicaSP5 confocal microscope on the ear dermis, as previously described(Auffray et al., 2007). Briefly, mice were anesthetized using a cocktail of ketamine (50 mg/kg), xylazine (10 mg/kg), and acepromazine (1.7 mg/kg) injected intraperitoneally and were kept at 37°C and received oxygen (0.5 l/min). Ears of reporter mice were taped to the center of the coverslip and 80 µL of TRITC conjugated 70kDa dextran (70µM) was injected intravenously, secondly purified human monocytes were injected I.V. Light was generated from 488-nm, 543-nm and 633-nm laser lines, and emitted light signals were detected to generate three-color 8-bit images, using a 20x/0.75 Plan Apochromat objective. Stacks of 3 squared x−y sections with 10 µm z spacing were acquired. Videos were generated using ImageJ software (v1.42, NIH, USA), by summing signal intensity from each stack of 3 squared x−y sections. Maximum projections (path tracks) were made on time-lapse series acquired containing images covering a 50 min period in the dermis both in the steady state and after adoptive transfer. LFA-1 has been previously been shown to be important in mediating mouse monocyte patrolling (Auffray et al., 2007) therefore we examined the role of LFA-1 in adoptively transferred CD14dim patrolling monocytes. After adoptive transfer of labelled CD14dim monocytes, steady state movies were initiated as described, before intravenous injection of 2mg/kg of antibodies (0.5mg/ml in Saline) blocking human LFA-

1(clone 38) or control antibody (clone X39). Images were acquired for at least 45mins post injection. Data presented are representative of calculated pathlengths using MetaMorph (Molecular Devices, USA), as previously described (Auffray et al., 2007) from 6 time-lapse series made on 2 *Rag-/-, γc-/- Cx3cr1gfp/+* mice for either $CD14^{+}CD16^{-}$ or $CD14^{dim}CD16^{+}$ adoptively transferred cells.

Array analysis

Samples: The human samples come from 3 different healthy donors (D1, D2, D3) but the samples from donor D1 are in triplicate. Twenty-five 'Whole Human Genome' chips were therefore obtained from 5 prospective subsets and 3 different donors, including triplicate samples from 1 donor. Samples obtained from D1 are s16, s17, s18, s19 (CD14+CD16-), s20, s21, s22 (CD14+CD16+), s23, s24, s25 ($CD14^{dim}$CD16-), s26, s27, s28 ($CD14^{dim}$CD16- Slan+), and s29, s30, s31 ($CD14^{dim}$CD16- Slan-). Samples from D2 are s32 (CD14+CD16-), s33 (CD14+CD16+), s34 ($CD14^{dim}$CD16-), s35($CD14^{dim}$CD16- Slan+), and s36 ($CD14^{dim}$CD16- Slan-). Samples from D2 are s37 (CD14+CD16-), s38 (CD14+CD16+), s39 ($CD14^{dim}$CD16-), s40($CD14^{dim}$CD16- Slan+), and s41 ($CD14^{dim}$CD16- Slan-).

Six 'Whole Mouse Genome' chips, from Ly6C+ and Ly6C- mouse monocyte subsets were generated as described (Auffray et al., 2007). Mouse samples Gr1.p1, Gr1.p12, and Gr1.p13, correspond to mouse Gr1+ monocytes and Gr1.m1, Gr1.m12, and Gr1.m13, correspond to mouse Gr1- monocytes. MIAME data are available at www.ebi.ac.uk/arrayexpress: Geissman_Miltenyi_Human, ArrayExpress accession: E-MEXP-2544
and Geissman_Miltenyi_Mouse : ArrayExpress accession: E-MEXP-2545

We submitted this series of expression arrays to an unsupervised analysis in order to unveil possible correspondences between samples from the two species. The two sets of data were obtained and processed independently.

Data sources: Data extraction and normalization was performed using the Feature Extractor Plug-In for GeneSpring GX software version 7.3 (Agilent Technologies) following the recommended Agilent Normalization Scenario for 1-Color Data. Two sets of, 25 Human (44k 012391 Whole Human Genome G4112A) and 6 Mouse (44k 012694 Whole Mouse Genome G4122A) Agilent chips have been processed independently. To eliminate the potential bias we performed the analysis using at first the independent triplicate (D1, D2, D3) and then their mean.

Common gene list: In a first part we have identified the common genes between the two types of chips (Ingenuity homolog mapping). The corresponding probes have been selected and grouped by gene using their mean to obtain one intensity measure by gene and by sample. We have selected common genes to both species.

Gene selection: Only genes showing for each species at least one n-fold variation of mean expression between two groups among all possible have been selected. By this way we focus our interest on group's specifics genes discarding invariants ones.

Intensity values replacement: To limit influence of specie specific gene expression level we choose to replace each intensity measure by the values "-1", "0" or "1". Each value was replaced according to their comparison with the median of all intensity measures of the corresponding gene considering the species independently. If the value was within an interval of 10% around the median we replace this value by "0", we replaced it by "-1" if it was lower than the interval and by "1" if it was higher.

Unsupervised analysis: We merged the Human and Mouse data sets and submitted it to a hierarchical clustering and a PCA. PCA was performed on covariance matrix.

The clustering was performed using the Spearman correlation similarity measure and average linkage in clustering algorithm. Separation between subsets is early visible using all the common genes despite of some errors (Supplemental Figure S1). If genes are filtered using a

2-fold variation there is no error in the classification (Figure 1F). Results from the hierarchical clustering analysis using D1, D2 and D3 with all individual D1 biological replicates (figure 1F), with the mean of D1 replicates (Supplemental figure S1), or with individual replicates (not shown) were similar and led to an identical conclusion.

Stimulation of monocytes.

$CD14^{high}CD16^{low}$, $CD14^{low}CD16^{high}$ and $CD14^{high}CD16^{high}$ cells were sorted from the blood of healthy controls, and MyD88 and IRAK deficient patients when indicated, as described above and diluted in 10% fetal calf serum/1% penicillin-streptomycin Opti-MEM® media to reach the desired concentration (10^5/ml). 10^4 cells/well were laid in a 96 well plate in 100microL, and stimulated with PBS control, TLR agonists, viruses, or human serum.

TLR agonists stimulations : Optimal concentration of TLR agonists were determined in preliminary experiments. In the experiments reported in this paper, the following concentration were used: LPS (TLR4 agonist) 1ng/ml, Pam3ck4 (TLR2) 100ug/mL, 3M2 (TLR8) 3µg/ml, R838 (TLR8) 3µg/ml, 3M13 (TLR7) 3µg/ml, in (10% FCS, 1%P/S) and incubated for 6, 24, or 48 hours at 37°C/5% CO_2. When indicated monocytes were preincubated (30mins) with the MEK inhibitor PD98059 (10-100µM), the P38 inhibitor SB-203580 (50µM), or DMSO vehicle control before exposure to TLR agonists.

Viral Stimulations. We stimulated 2 x 104 monocytes or PBMCs per well from controls and, when indicated from MYD88-deficient and IRAK-4-deficient patients, with the following intact viruses: ss(−)RNA (vesicular stomatitis virus [VSV, strain Indiana], measles virus [strain Edmonton], ss(+)RNA encephalomyocarditis virus [EMCV], and dsDNA (herpes simplex virus-1 [HSV-1, strain KOS-1] (Yang et al., 2005). VSV, MV, EMCV and HSV-1 were added at an moi of 1 and placed on ice for 30 minutes to obtain a synchronous infection. We treated were incubated for 18- 24hr at 37°C/5% CO_2. Cell supernatant was collected after a brief centrifugation and analyzed for cytokine production using the Biorad® multiplex assay or ELISA tests.

Infection of monocytes with HSV-1. HSV-1 gB-GFP (Flore Rosenberg). Triplicate of 20 000 sorted monocytes from each subsets were challenged with HSV-1 gB-GFP (kindly provided by Flore Rozenberg, Hopital Cochin - St-Vincent de Paul, Universite Paris-Descartes, flore.rozenberg@svp.aphp.fr) at a MOI of 1. Mock-infections were performed with heat-inactivation (60°C for 30 minutes) by UV-inactivation (Germicide UV-lamp for 30 minutes) of the same viral stock and with media only. HSV-1 permissive human fibroblasts (MRC5) were infected in parallel as a positive controls. Cells were analyzed for GFP fluorescence 18 hours after infection using a Cyan flow cytometer (Dako).

Human serum: was obtained under informed consent from patients Systemic lupus erythematosus patients diagnosed according to the BILAG criteria in the Lupus clinic within St Thomas Hospital at KCL, London. Blood from patient and controls was collected and serum prepared and stored at -80oC. Serum was analyzed for anti-SS RNA/protein antibody (RNP) and anti-dsDNA auto-antibodies using the Crithidia test. Anti-RNP and anti-DNA titers were determined. Three patients positive for antibodies against RNP, 1 patient without detectable auto-antibody (disease control, control 1) and a healthy volunteer (control 2) were selected. In order to insure generation of immune complexes capable of activating monocytes in some experiments serum was spiked with RNP antigen (2µg/ml, Arotec Diagnostics). In some experiments all immunoglobins were depleted by incubating serum samples with Protein A bead (0.25mg/ml, Millipore) according to manufacturers instructions.

Immunodepletion of immunoglobulins was confirmed through ELISA. Further in some experiments RNA and DNA was depleted by treating serum with RNAse and DNAse (2units, Sigma) for 6 hours at 4oC before each experiment. $CD14^{low}CD16^{high}$ monocytes were sorted into 140µl of 20% resting or treated serum samples in 96 well plates maintained at 4oC.

Cytokine measurements: After 24 hours plates were centrifuged and supernatant collected at stored at -80 ^{O}C until cytokine measurement.
Type-I IFN was measured as described (Yang et al., 2005).Other cytokines were measured using Elisa when indicated, or more frequently using the BioRad® BioPlex human cytokine kit according to manufacturers instructions. Bead fluorescence emission was detected using the Luminex LX100 multiplex system (Luminex Corporation) and data analyzed using STarStation3.0 (AppliedCytometry) according to manufacturers instructions. The following cytokines were measured IL1b, IL1-RA, IL2, IL4, IL5, IL6, IL7, IL8, IL9, IL10, IL12, IL13, IL15, IL17, TNF, CCL3 (MIP1a), MIP1b, CCL11, FGFb, IFNg, IP10, CCL5 (Rantes), G-CSF, GM-CSF, MCP-1, and PDGF and VEGF. Data are presented as pg/ml of each cytokine.

Protein phosphorylation: Phosphorylated intracellular signaling proteins (Akt-P, CREB-P, ERK1-2 –P, GSKα-P, JNK-P, MEK1-P, P38-MAPK-P) was analysed using the BioRad Bio-Plex phosphoprotein detection kit according to manufacturers instructions. Briefly, FACS sorted $CD14^{high}CD16^{low}$, $CD14^{low}CD16^{high}$ monocytes were stimulated with TLR agonists or vechile control as above (see *stimulation with TLR agonists* and *cytokine measurement*) for 0, 30 or 120mins and subsequently cell lysates prepared using manufactures lysis buffer containing PMSF. Lysate protein concentration was then determined in each sample using BioRad's DC protein assay. Each lysate was equilibrated to 200µg/ml to load equal amounts of protein for each measurement. Bead fluorescence emission was detected using the Luminex LX100 multiplex system (Luminex Corporation) and data analysed using STarStation3.0 (AppliedCytometry) as above. Data is presented as mean fold change in phosphorylated protein levels from control treated samples.

Infection of monocytes with HSV-1. HSV-1 gB-GFP (Flore Rosenberg). Triplicate of 20 000 sorted monocytes from each subsets were challenged with HSV-1 gB-GFP (kindly provided by Flore Rozenberg, Hopital Cochin - St-Vincent de Paul, Universite Paris-Descartes, flore.rozenberg@svp.aphp.fr) at a MOI of 1. Mock-infections were performed with heat-inactivation (60°C for 30 minutes) by UV-inactivation (Germicide UV-lamp for 30 minutes) of the same viral stock and with media only. HSV-1 permissive human fibroblasts (MRC5) were infected in parallel as a positive controls. Cells were analyzed for GFP fluorescence 18 hours after infection using a Cyan flow cytometer (Dako).

phagocytosis assay: Monocyte, DR- cells and NKp46 NK cells were incubated with 1.0 µm biotinylated YG-Fluospheres ($1.3*10^{10}$ particles/ml),in prewarmed (37°C) KRP buffer for 10, 20 or 30 min at 37°C. Cells were then adiluted with 3 ml cold PBS, spin 5 min, 350x g, 4ºC and phagocytosis was measured by flow cytometry after incubation with streptavidin-pacific blue. YG positive, pacific blue negative cells, have phagocytosed beads.

ROS production : FcOxyburst reagent (FcO) consists of IgG-opsonised BSA that has been labelled with H2DCF (dichlorodihydrofluorescein). ROS production was investigated after incubation with 80 µg/ml of FcO for 10 min at 37°C. H2DCF oxidation results in the formation of green fluorescent DCF (dichlorofluorescein). DCF peak fluorescence intensity (MFI) for is measured by flow cytometry for each population after 10 min at 37°C.

Antigen presentation assay: Blood monocytes subsets, blood DCs, and autologous T cells are purified from blood by flow cytometry from an tetanos toxoid-immunized healthy donor and incubated with or without tetanos toxoid and LPS for 4 days. IL2 is measured in the supernatant after 4 days. Thymidine incorporation is measured during the last 18h. In contrast to DCs, monocytes do not stimulate proliferation of T cell to the recall antigen (tetanos toxoid) and do not trigger IL2 production. Experiment representative of 5 on different donors.

Histology: Patients, antibodies, staining protocols, cell counts
Tissue samples from patients with Lupus nephritis (n=3) were obtained after informed consent according to institutional regulation after informed consent. IHC was performed on paraffin sections cut at 2 to 3 μm and baked for 4 hours at 60°C. Slides were deparaffinized in xylene and brought to water through graded ethyl alcohol. Endogenous peroxidase activity was quenched by treating slides with 0.5% hydrogen peroxide in methyl alcohol for 10 minutes. Heat-induced epitope retrieval was performed on the slides using 0.01 mol/L citrate buffer, pH 6.0. After heating for 40 minutes, cooling, and washing in 0.01 mol/L phosphate-buffered saline, slides were incubated in primary antibody for 45 minutes: CD3ε (polyclonal rabbit A0452, 1/250, DAKO, Glostrup, DK), CD68 (monoclonal mouse KP1, 1/3000, DAKO, Glostrup, DK), CD16 (monoclonal mouse CD16, 1/100, Newcastle, Novocastra, UK), CD14 (monoclonal mouse CD14-223, 1/100, Newcastle, Novocastra, UK), CD5 (monoclonal mouse 4C7, 1/50, Newcastle, Novocastra, UK). Sections were washed 2x5 minutes in 0.01 mol/L phosphate-buffered saline and incubated with link biotinylated secondary antibodies (sol A, Dako K5001) for 30 minutes, washed 2x5 minutes in 0.01 mol/L phosphate-buffered saline and incubated with streptavidin peroxidase (sol B, Dako K5001) for 30 minutes. Sections were washed 2x5 minutes in 0.01 mol/L phosphate-buffered saline and incubated with Diaminobenzidine and hydrogen peroxide for 10 minutes. Slides were counterstained with hematoxylin.

Computational Modeling of TLR7/8 signalling

A computational model was constructed to examine toll-like receptor 7 and 8 (TLR7/8) signaling and to ascertain the roles of MAP kinases p38, MEK1 (and its target, ERK) and JNK in regulating cytokine production in different monocyte subsets (Sup Figure 4). The mathematical model consists of a system of ordinary differential equations (ODE) with mass action kinetics and rate constants, where each ODE represents a component in the pathway. To reduce complexity, some multi-step reactions were combined into single reaction mechanisms, represented by Monod and competitive inhibition kinetics. These equations were written and solved with MATLAB® version R2009b (The MathWorks) using the *ode23* solver at default settings.
A controlled perturbation was introduced to the input component of the system (TLR7/8), to monitor the response of the output components (cytokines and MAP kinases) from steady-state. The experimental data shown in Figures 4, 5 and S3, were used as training data for parameter optimization to fine-tune the model. Simulations for the various outputs are shown in supplementary Figure S4. In silico inhibition of different p38 and MEK1 was also performed to see its impact on cytokine simulation (supplementary Figure S4). Reaction equations and parameter values for the model are available upon request.

Supplemental References for Supplemental Experimental Procedures

Auffray, C., Fogg, D., Garfa, M., Elain, G., Join-Lambert, O., Kayal, S., Sarnacki, S., Cumano, A., Lauvau, G., and Geissmann, F. (2007). Monitoring of blood vessels and tissues by a population of monocytes with patrolling behavior. Science *317*, 666-670.

Yang, K., Puel, A., Zhang, S., Eidenschenk, C., Ku, C. L., Casrouge, A., Picard, C., von Bernuth, H., Senechal, B., Plancoulaine, S., *et al.* (2005). Human TLR-7-, -8-, and -9-mediated induction of IFN-alpha/beta and -lambda Is IRAK-4 dependent and redundant for protective immunity to viruses. Immunity *23*, 465-478.